ACS Partner Journal

CHEMICAL & BIOMEDICAL IMAGING

pubs.acs.org/ChemBioImaging

Article

Development of an *In Vitro* Assay for Evaluation of Intracellular SPAAC Reactions Using Hoechst-DBCO

Luciana Kovacs, Risto Savela, Jelena Matovic, Tatsiana Auchynnikava, Filip S. Ekholm, and Anu J. Airaksinen*

Cite This: https://doi.org/10.1021/cbmi.5c00207

Read Online

ACCESS | Metrics & More | Article Recommendations | Supporting Information

ABSTRACT: Strain-promoted azide−alkyne cycloaddition (SPAAC) reactions between azides and strained alkynes are some of the most widely used bioorthogonal reactions for molecular imaging applications, such as in positron emission tomography (PET). Radiolabeled azides and alkynes have been developed for click reactions; however, very few compounds have been studied in the intracellular space, where stability, selectivity, and reactivity may be affected by the surrounding complex intracellular environment. Motivated by the lack of tools to evaluate azide tracer candidates for bioorthogonal click reactions in the intracellular compartment, we designed and synthesized Hoechst-DBCO, a Hoechst 33258 derivative that accumulates in cells. Hoechst 33258 has strong DNA binding properties and is used as a courier to deliver dibenzocyclooctyne (DBCO), a strained alkyne, into the nucleus to track click reactions in living cells. The ultimate aim of this study was to develop an *in vitro* assay to detect and investigate specific SPAAC bioorthogonal click reactions in living cells and to evaluate permeability, uptake, and reactivity in the intracellular compartment. The Hoechst-DBCO compound we developed can help accelerate the evaluation of candidates for bioorthogonal click reactions and find suitable radiopharmaceuticals for imaging procedures.

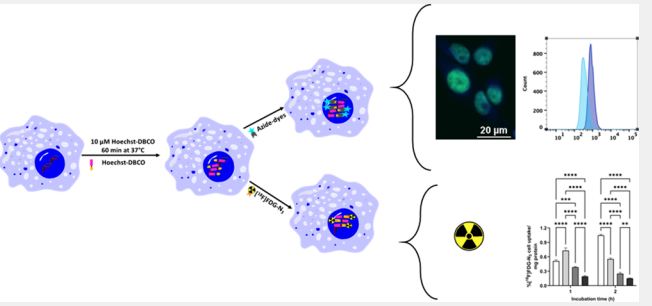

KEYWORDS: *Hoechst 33258, bioorthogonal click reaction, SPAAC, intracellular reaction, pretargeted PET imaging*

INTRODUCTION

Bioorthogonal click chemistry defines a set of chemical reactions that can occur in biological systems without interfering with known biochemical processes. These reactions provided important advances over the past two decades in biomedical research, including drug development, biomolecule labeling, nanoscience, and radiochemistry.[1−8] These innovative methods have revolutionized the way scientists study interactions between biomolecules in their native environments. The significant influence of click chemistry on the chemical and biological sciences was widely recognized even prior to the Nobel Prize in Chemistry 2022, which was awarded to Bertozzi, Meldal, and Sharpless.[9] Bioorthogonal click reactions are a valuable tool in radiopharmaceutical chemistry, offering selectivity, efficiency, simplicity, and biocompatibility, essential characteristics for effective radiopharmaceutical synthesis.[10] At the same time, they enable the development of new approaches in radiochemistry, including the use of prosthetic groups for radiolabeling reactions and the development of pretargeted positron emission tomography (PET) imaging.[11]

Among the bioorthogonal click reactions, SPAAC reactions have gained popularity in chemical biology. SPAAC reactions were first introduced by Bertozzi in 2004 as a solution to the primary constraint of copper-catalyzed azide−alkyne cycloaddition (CuAAC) ligations: their dependence on a copper catalyst, which limits the compatibility of the reaction in various biological environments. The SPAAC reaction is based on a covalent bond formation between an azide and a strained alkyne, such as cyclooctynes, to form a stable triazole.[12] SPAAC proceeds with second-order kinetics, has reaction rate constants of ∼1−10^6 M^{-1} s^{-1},[9] and occurs under aqueous conditions without a catalyst at room temperature.[13]

As bioorthogonal labeling strategies become more prevalent, so do the potential applications within the field of radiopharmaceutical chemistry. In more detail, various techniques have been employed to incorporate bioorthogonal groups into biomolecules, enabling the examination of bioorthogonal click reactions in an intracellular context. Protocols including enzymatic ligation, metabolic labeling, covalent inhibition with clickable inhibitors, and genetic encoding fusion proteins,

Received: October 27, 2025
Revised: November 27, 2025
Accepted: December 15, 2025
Published: December 29, 2025

such as the engineered haloalkane dehalogenase known as Halo Tag and the covalent self-labeling O^6-alkylguanine-DNA alkyltransferase known as SNAP Tag, have all been reported in the literature.[14−18] These proteins engage in covalent interactions with small molecules, facilitating targeted and selective labeling in living systems. However, the tags are large and can impede the trafficking and function of fused proteins.[14,16] Other methods, such as sortase, aldehyde tag, and short peptide tags S6 and A1 (Sfp/AcpS), are restricted to labeling of cell surface proteins.[19] While the aforementioned techniques are valuable to the scientific community, the protocols are expensive and demanding to use. Consequently, there seems to be a lack of practical methods that can be utilized to assess cellular uptake and click reactions in the intracellular space, where permeability and selectivity are factors to be considered. The development of such methods is a must for radiopharmaceutical imaging.

In the present study, we designed and synthesized a small molecule that would deliver a bioorthogonally clickable functional group into the cell nucleus, thereby providing a sound platform for assessment of intracellular click reactions in living cells. The backbone of choice was Hoechst 33258, a bisbenzimidazole dye. Hoechst 33258 enters cells and accumulates within the nucleus due to its high affinity for DNA. In addition, it displays good cellular permeability, high selectivity, and low cytotoxicity and can be produced with low manufacturing cost. To allow assessment of intracellular SPAAC reactions, Hoechst 33258 was further conjugated to DBCO via a linker that would not significantly affect the desirable properties of the parent molecule. In this study, we report on the potential of the Hoechst-DBCO conjugate for assessing intracellular click reactions. We show the design and synthesis of Hoechst-DBCO, analysis of cellular uptake, and the click reaction with three commercially available azides (boron-dipyrromethene (BDP) FL azide, tetramethylrhodamine (TAMRA) azide (5-isomer), and sulfo-cyanine 5 (Cy5) azide) using a fluorescence assay, fluorescence microscopy, and flow cytometry. The azides were selected based on their cell permeability profiles. BDP FL azide and TAMRA azide (5-isomer) present favorable physicochemical properties and high membrane permeability, while sulfo-Cy5 azide is hydrophilic and shows low cell permeability. Overall, we develop and validate a new tool for assessing intracellular click reactions with direct applications within radiopharmaceutical chemistry and imaging.

MATERIALS AND METHODS

General Considerations

Chemicals and solvents for the synthesis of Hoechst-DBCO (**2**) were purchased from Merck, ABCR, and BroadPharm and used without further purification. Precursor (**1**) to Hoechst-DBCO (**2**) was prepared according to published procedure from 2′-(4-hydroxyphenyl)-5-(4-methyl-1-piperazinyl)-2,5′-bi(1H-benzimidazole) trihydrochloride hydrate (Hoechst 33258), with matching analytical data.[20] Reactions were followed using thin-layer chromatography (200 μm silica gel 60 F_{254} on aluminum plate) and purified using amine-functionalized silica (particle size: 20−40 μm, pore size 100 Å, and mesh size 400−632). For characterization of compounds, a Bruker Avance-III spectrometer operating at 500.12 MHz (^{1}H) and 125.74 MHz (^{13}C) equipped with a Smartprobe BB/1H and Bruker Avance-III spectrometers operating at 600.16 MHz (^{1}H) and 150.91 MHz (^{13}C) equipped with a Prodigy TCI CryoProbe were used. The characterization was performed using a standard set of 1D and 2D NMR spectroscopic techniques: ^{1}H, ^{13}C, COSY, multiplicity-edited HSQC (CH and CH_3 positive, CH_2 negative, both coupled and decoupled), and HMBC and H2BC. CAL27 (CRL-2095) and HEK293 (CRL-1573) cell lines were purchased from American Type Culture Collection (ATCC, Manassas, USA). Dulbecco's Modified Eagle Medium (DMEM), fetal bovine serum (FBS), penicillin−streptomycin (catalog no.: 15070-063), Trypsin/EDTA (0.25%), and phosphate-buffered saline (PBS) were purchased from Life Technologies, Gibco, Carlsbad, CA, USA. Trypan blue (1450021) was purchased from Bio-Rad (Hercules, California, USA). Cell culture flasks (75 cm^3) and six-well plates were purchased from Corning (Glendale, Arizona, USA). Prolong Diamond Antifade Mountant was purchased from Invitrogen (Waltham, MA, USA). Phalloidin-iFluor 594 (ab176757) was purchased from Abcam (Cambridge, UK). BDP FL azide (BP-22542) was purchased from BroadPharm (San Diego, CA, USA). TAMRA azide (5-isomer) (A7130) and sulfo-Cy5 azide (A3330) were purchased from Lumiprobe (Hannover, Germany). WST-1 Cell Proliferation Assay Kit was purchased from Cayman Chemical (Michigan, USA). Pierce BCA protein assay was purchased from Thermo Fischer Scientific, Waltham, MA, USA. Quick Start Bradford protein assay was purchased from Bio-Rad, Hercules, California, USA.

(11,12-Didehydro-y-oxodibenz[*b,f*]azocine-5-(6*H*))-*N*-(4-(4-(5-(4-methyl-1-piperazinyl)[2,5′ bibenzoimidazol]-2′-yl)phenoxy)butyl)-6-oxohexanamide (2)

Compound **1** (16.5 mg, 27.5 μmol) was suspended in dichloromethane (0.8 mL), followed by the addition of trifluoroacetic acid (0.2 mL, 3 mmol). The suspension turned quickly into a yellow homogeneous solution, and it was stirred for 3 h at room temperature. The mixture was evaporated under reduced pressure and then co-evaporated from methanol three times (2 mL each) to afford a yellow oil. The oil and 4-(dimethylamino) pyridine (20.3 mg, 166 μmol) were suspended in *N*,*N*-dimethylformamide (0.5 mL). A solution of 2,5-dioxo-1-pyrrolidinyl 11,12-didehydro-ε-oxodibenz[*b,f*]azocine-5(6*H*)-hexanoate (11.9 mg, 27.7 μmol) in *N*,*N*-dimethylformamide (0.6 mL) was added dropwise to the suspension. The reaction mixture was stirred overnight at room temperature and then loaded directly onto Celite. The product was purified by flash chromatography (gradient 0−15% MeOH in $CHCl_3$), using amine-derivatized silica, yielding a waxy white solid after evaporation of solvents. Yield: 16 mg, 71%. R_f = 0.36 (10% MeOH in $CHCl_3$).

^{1}H NMR (500.12 MHz, $CDCl_3$) δ 8.33 (br, 1H), 7.82 (br, 1H), 7.68 (br, 2H), 7.57 (d, J = 7.3 Hz, 1H), 7.40 (br, 1H), 7.36−7.12 (m, 9H), 6.72 (br, 2H), 6.41 (br, 2H), 5.06 (d, J = 13.9 Hz, 1H), 3.60 (d, J = 13.9 Hz, 1H), 3.55 (br, 1H), 3.09−2.90 (m, 6H), 2.48 (br, 4H), 2.27 (s, 3H), 2.19−2.13 (m, 1H), 1.90−1.79 (m, 3H), 1.50 (br, 2H), 1.45−1.27 (m, 4H), 1.27−1.15 (m, 2H).

^{13}C NMR (125.74 MHz, $CDCl_3$) δ: 173.6, 173.2, 160.3, 153.9, 152.5, 151.6, 148.1, 132.3, 129.1, 128.6, 128.32, 128.25, 127.8, 127.2, 125.5, 124.0, 123.1, 122.5, 121.6, 121.4, 115.0, 114.5, 108.0, 67.3, 55.6, 55.3, 50.7, 46.1, 39.0, 36.0, 34.5, 26.5, 26.1, 25.0, 24.6. HRMS-ESI: m/z $[M + Na]^+$ calcd. for $C_{50}H_{50}N_8O_3Na$: 833.3898, found 833.3897.

Radiosynthesis of [^{18}F]FDG-N_3 (2,6-Dideoxy-6-azido-2-fluoro-D-glucose)

[^{18}F]FDG-N_3 was synthesized from the corresponding trifluoromethanesulfonyl precursor (6-deoxy-6-azido-1,3,4-tri-*O*-acetyl-2-*O*-trifluoromethanesulfonyl-β-D-mannopyranoside), as reported by Auchynnikava et al.[21]

Cell Culture

The human tongue squamous cell carcinoma cell line CAL27 and human embryonic kidney (HEK) 293 cells were cultured in DMEM medium supplemented with 10% FBS. Cells were cultured in a humidified atmosphere containing 5% CO_2 at 37 °C. Cells were detached with Trypsin/EDTA (0.25%) and counted with Trypan blue.

https://doi.org/10.1021/cbmi.5c00207
Chem. Biomed. Imaging XXXX, XXX, XXX−XXX

Fluorescence Microscopy

CAL27 and HEK293 cells were seeded on 20 mm coverslips in six-well plates at a density of 20,000 cells per well and cultured for 48 h at 37 °C in a humidified atmosphere with 5% CO_2. The cells were incubated with 1, 2, 3, 5, and 10 μM Hoechst-DBCO or with 10 μM Hoechst 33258 in DMEM media with 2% FBS for 15, 30, and 60 min at 37 °C. 2% FBS was used to reduce background binding and improve signal. Following incubation, the cells were washed twice with PBS and fixed with 4% paraformaldehyde (PFA) in PBS for 15 min at room temperature. For actin staining, the cells were permeabilized with 0.1% Triton X-100 in PBS for 5 min at room temperature, washed twice with PBS, and then incubated with 165 nM Phalloidin-iFluor 594 in PBS with 1% BSA for 20 min at room temperature. The cells were washed twice with PBS, and slides were mounted with Prolong Diamond Antifade Mountant.

To evaluate the click reaction, cells were initially incubated with 10 μM Hoechst-DBCO for 1 h at 37 °C and then washed 3 times with PBS. 1 μM BDP FL azide, 1 μM TAMRA azide (5-isomer), or 1 μM sulfo-Cy5 azide in DMEM with 2% FBS was added, and the cells were incubated for 60 min at 37 °C. As a control experiment, cells were pretreated with 10 μM Hoechst 33258 for 60 min at 37 °C, followed by incubation with the dyes as described above. Additional controls included cells treated with 1 μM BDP FL azide, 1 μM TAMRA azide (5-isomer), or 1 μM sulfo-Cy5 azide alone for 60 min at 37 °C, followed by actin staining with Alexa Fluor 594 phalloidin as described above. After incubation, the cells were washed twice with PBS, fixed with 4% PFA for 15 min at room temperature, and washed twice with PBS. Coverslips were mounted with Prolong Diamond Antifade Mountant. Fluorescence images were acquired using a Nikon Eclipse Ti2-E microscope and processed with Nikon NIS-Elements AR software (version 5.11.01).

Flow Cytometry

Flow cytometry was performed using CAL27 and HEK293 cells. 1×10^6 cells were suspended in 100 μL of DMEM supplemented with 2% FBS and 2.5, 5, or 10 μM Hoechst-DBCO or 10 μM Hoechst 33258. The cells were incubated for 60 min at 37 °C, then washed three times with PBS, centrifuged at 300*g* for 5 min, and resuspended in PBS with 2% BSA. For click reaction analysis, cells pretreated with 10 μM Hoechst-DBCO and untreated cells were treated with 1, 2.5, 5, and 10 μM BDP FL azide, followed by incubation for 60 min at 37 °C. As an additional control, the cells treated with 10 μM Hoechst 33258 were incubated with 10 μM BDP FL azide under the same conditions. Following incubation, the cells were washed three times with PBS, centrifuged at 300*g* for 5 min, and resuspended in PBS with 2% BSA. Cellular fluorescence was measured by flow cytometry using an LSRFortessa (BD) cytometer and BD FACS Diva software. Each experiment was performed in triplicate. Data were analyzed using FlowJo software.

Bioorthogonal Click Reaction *In Vitro* Assay

Lysis Conditions. Several conditions were evaluated to optimize the cell lysis solution and find conditions for the complete recovery of Hoechst-DBCO fluorescence for accurate quantification. Sodium dodecyl sulfate (SDS) and 100× Triton were tested as detergents in 10 and 20 mM phosphate buffer (pH 7) or Tris buffer (pH 7) containing 0.15 mM NaCl. 1×10^6 cells in 100 μL of PBS were transferred to an Eppendorf tube and centrifuged at 300*g* for 5 min. The supernatant was discarded, and 500 μL of different lysis buffers containing 0.5 μM Hoechst-DBCO were added to the pellet. Samples were sonicated for 3 min and centrifuged at 14,000*g* for 10 min to pellet cell debris. Control experiments were performed in the absence of cells. Fluorescence in the supernatant was analyzed by using a Synergy H1 Hybrid Reader, BioTek, with an excitation wavelength of 352 nm, an emission wavelength of 400−600 nm, and an acquisition duration of 0.2 s/0.7 nm.

***In Vitro* Cellular Uptake Analysis of Hoechst-DBCO.** 5×10^5 CAL27 cells/well were seeded in a 6-well plate. The cells were incubated for 24 h at 37 °C with 5% CO_2 in a humidified atmosphere. After 24 h, the media were removed, the cells were washed twice with PBS, and 2.5, 5, or 10 μM Hoechst-DBCO in 1 mL of DMEM media with 10% FBS was added per well in triplicate. The cells were incubated for 1 h at 37 °C and then washed three times with PBS. 1 mL of DMEM media with 10% FBS was added to the cells and incubated for 1 h at 37 °C, with two media changes to remove unbound Hoechst-DBCO. Then, the cells were washed three times with PBS, and 600 μL of lysis buffer (0.15 mM NaCl + 1% SDS in 20 mM phosphate buffer, pH 7) was added per well.

***In Vitro* Cellular Uptake Analysis of Dye-Conjugated Azides.** For the SPAAC reaction, CAL27 cells pretreated with 2.5 or 10 μM of Hoechst-DBCO and untreated cells were treated with 10 nM−100 μM BDP FL azide, and cells pretreated with 10 μM of Hoechst-DBCO and untreated cells were treated with 10 nM−100 μM TAMRA azide (5-isomer) or sulfo-Cy5 azide in 1 mL of DMEM media with 10% FBS for 1 h at 37 °C. The cells were washed three times with PBS, and 1 mL of DMEM media with 10% FBS was added to the cells and incubated for 1 h at 37 °C, with two media changes to remove unbound azides. Then, the cells were washed three times with PBS, and 600 μL of lysis buffer was added per well. Samples were sonicated for 3 min and centrifuged at 14,000*g* for 10 min. 100 μL of supernatant was transferred to a black 96-well plate in triplicate. The same lysis conditions used for Hoechst-DBCO measurements were applied to the three azides in this study. For cellular uptake studies of Hoechst-DBCO and dye-conjugated azides, DMEM with 10% FBS was used to support cell viability and maintain physiological conditions during the longer incubation periods. The assay was performed in triplicate.

The uptake of compounds by CAL-27 cells was quantified through direct fluorescence measurement of the supernatant. The concentration of each compound was determined using a calibration curve based on the fluorescence intensity of known amounts of Hoechst-DBCO, BDP FL azide, TAMRA azide (5-isomer), and sulfo-Cy5 azide present in the cell lysates, which were performed simultaneously for each experiment. A calibration curve without cells was included in each experiment as a control for the standard curve obtained with the cells.

For the calibration curve, different concentrations of Hoechst-DBCO, BDP FL azide, TAMRA azide (5-isomer), or sulfo-Cy5 azide were added to 1×10^6 cells suspended in 600 μL of lysis buffer. The samples were sonicated for 3 min and centrifuged at 14,000*g* for 10 min. 100 μL of supernatant was transferred to a black 96-well plate in triplicate. The fluorescence intensity in the supernatant was measured with a plate reader (Synergy H1 Hybrid Reader, BioTek). Fluorescence spectra were acquired for Hoechst-DBCO (excitation: 352 nm, emission: 495 nm), BDP FL azide (excitation: 485 nm, emission: 520 nm), TAMRA azide (5-isomer) (excitation: 530 nm, emission: 580 nm), and sulfo-Cy5 azide (excitation: 640 nm, emission: 670 nm). The protein concentration of each sample was determined using Pierce BCA Protein assay kits, as recommended by the manufacturer. A summary of the steps for the cell lysate quantification method is presented (Scheme 1).

Scheme 1. Quantification Method for the Cell Lysate

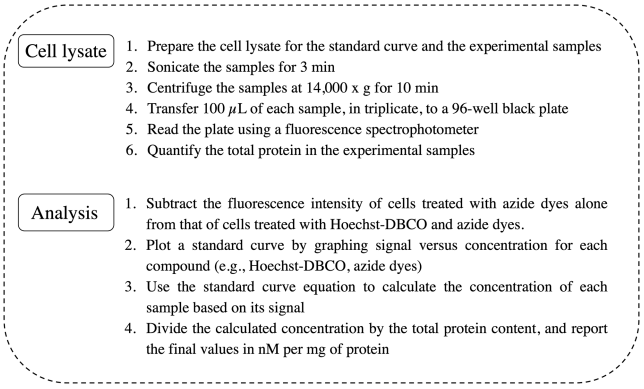

https://doi.org/10.1021/cbmi.5c00207
Chem. Biomed. Imaging XXXX, XXX, XXX−XXX

Scheme 2. Synthesis of Hoechst-DBCO (2) from Hoechst 33258[a]

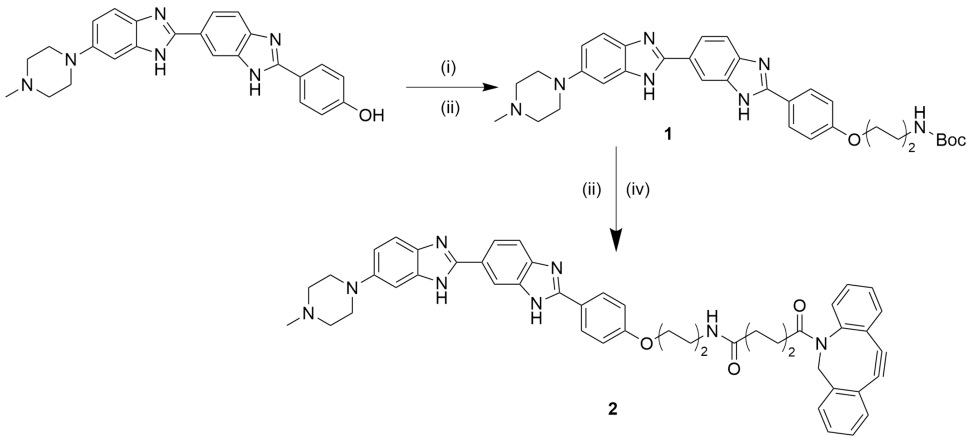

[a](i) K_2CO_3, H_2O (ii) K_2CO_3, DMF, 4-(Boc-amino)butyl bromide; yield 55% over (i, ii). (iii) TFA, dichloromethane and (iv) DMAP, DBCO-C6-NHS, dichloromethane; yield 71% over (iii, iv).

***In Vitro* Cellular Uptake Analysis of [^{18}F]FDG-N_3.** Cells pretreated with 10 μM Hoechst-DBCO were washed twice with PBS; 1 mL of glucose-free DMEM was added per well, and the plates were incubated for 10 min at 37 °C. The medium was removed, and 0.5 MBq [^{18}F]FDG-N_3 in 1 mL of glucose-free DMEM was added to each well of cells pretreated with 10 μM Hoechst-DBCO and untreated cells. The cells were incubated for 60 and 120 min at 37 °C. Competition studies with fluorodeoxyglucose (FDG) were performed. The media were removed, and 0.5 MBq [^{18}F]FDG-N_3 in 1 mL of glucose-free DMEM with 18 nM FDG (cold) was added to cells pretreated with 10 μM Hoechst-DBCO. The cells were incubated for 60 and 120 min at 37 °C. A targeted approach was also performed, and Hoechst-DBCO was mixed with [^{18}F]FDG-N_3 in 100 μL media and incubated for 2 h at room temperature. The amount of Hoechst-DBCO and [^{18}F]FDG-N_3 used was calculated for a final concentration of 10 μM Hoechst-DBCO and 0.5 MBq [^{18}F]FDG-N_3 /mL at the time the solution was added to the cells. The media were removed, and 0.5 MBq [^{18}F]FDG-N_3-DBCO-Hoechst in 1 mL of glucose-free DMEM was added per well and incubated for 60 and 120 min at 37 °C. After the incubation time, the solution was removed and transferred to a scintillation tube. The cells were washed with 1 mL of ice-cold PBS, and the solution were transferred to the same scintillation tube. The cells were then washed twice with 1 mL ice-cold 0.05 M glycine buffer containing 0.15 M NaCl (pH 2.8) to detach any surface-bound activity and washed one time with PBS; the solution was then transferred to a new scintillation tube. 0.3 mL/well of 1 M NaOH was added to the cells and incubated for 10 min at room temperature. The cell lysate was collected in a new scintillation tube, and the wells were washed twice with 0.85 mL of PBS and collected in the same tube. Radioactivity in the incubation solution, washed solution, and cell lysates was measured using a 2480 automatic gamma counter Wizard2 3" (PerkinElmer, Waltham, MA, USA). The percent uptake was normalized with total added activity and calculated as % uptake = 100 × CPM of uptake fraction/SUM of the CPM in all fractions. The assay was performed in triplicate. Total protein concentration in the samples was determined using Quick Start Bradford protein assay following the manufacturer's protocol. Data were calculated as percent of radiotracer uptake per mg of protein (% uptake [^{18}F]FDG-N_3/mg protein).

RESULTS AND DISCUSSION

Design and Synthesis of Hoechst-DBCO

Hoechst dyes are well-known for being readily transported into and tolerated by living cells. In addition, they represent a substrate class that is readily available at a competitive price for most end users. While the Hoechst dyes bind with high affinity to the minor groove of the DNA and localize mainly in the nucleus, it has been shown that structural analogues with long linkers (12 atoms and above) exhibit a more heterogeneous distribution, with increasing amounts also found in the extranuclear space.[22] As mentioned above, these factors led us to select Hoechst 33258 as the backbone structure to which an 11-atom linker ending with a strained alkyne (DBCO) was attached.

The Hoechst-DBCO probe was synthesized in three steps from Hoechst 33258 trihydrochloride hydrate, as illustrated in Scheme 2. The hydrochloride salts were removed from H33258 with potassium carbonate in aqueous media, followed by a substitution reaction with 4-(Boc-amino)butyl bromide. Subsequently, the Boc-protection groups were removed with trifluoroacetic acid (TFA), and the resulting TFA salt was reacted with the DBCO-C6-NHS ester in the presence of 4-(dimethylamino) pyridine (DMAP) to form the Hoechst-DBCO conjugate **2** with 39% yield over 4 steps.

Hoechst-DBCO Localization within Cells

Fluorescence microscopy was used to study the cellular uptake of Hoechst-DBCO. This is possible because the dye exhibits increased fluorescence upon binding to DNA. To determine the optimal Hoechst-DBCO concentration and incubation time, we performed a series of microscopy experiments. After analyzing various concentrations and incubation times, 10 μM Hoechst-DBCO incubated for 60 min provided a clear and well-defined nuclear visualization. Figure S1 presents the results of CAL27 cells treated with 2, 5, and 10 μM Hoechst-DBCO and incubated at 37 °C for 60 min. Fluorescence microscopy was also used to assess the cellular localization of Hoechst-DBCO. Figure 1 shows CAL27 and HEK293 cells stained with Hoechst-DBCO and actin, as well as CAL27 cells stained with Hoechst 33258 and actin serving as a comparative control. The results indicate that Hoechst-DBCO localizes exclusively to the nucleus.

We note that the results are in agreement with the previous study by Ranjan et al., who analyzed the effects of linker lengths and composition on the cell permeability of Hoechst 33258.[22] According to both that study and our own, a Hoechst 33258 conjugate featuring a linker of 11 atoms or below is indeed localized in the nucleus. Moreover, quantification of cellular fluorescence after treatment with Hoechst 33258 and

https://doi.org/10.1021/cbmi.5c00207
Chem. Biomed. Imaging XXXX, XXX, XXX−XXX

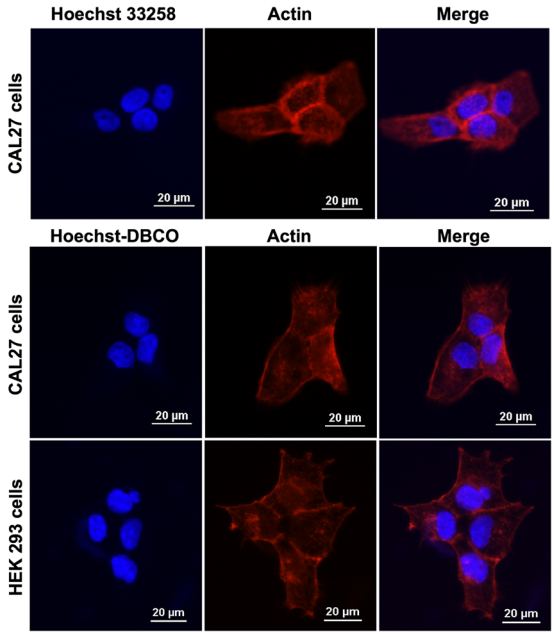

Figure 1. Cellular localization of Hoechst-DBCO. HEK293 and CAL27 cells treated with Hoechst 33258 or Hoechst-DBCO (blue), actin (red), and Hoechst/actin overlay to delineate the cellular localization. For actin staining, Alexa Fluor 594 phalloidin was used. Scale bars: 20 μm.

Hoechst-DBCO allowed determination of the effects of our chosen linker on cellular uptake.

Flow Cytometry

After observing differences in the distribution and fluorescence intensity by microscopy, we followed up with a flow cytometric assessment of the cellular uptake of Hoechst-DBCO at the single-cell level. CAL27 and HEK293 cells were treated with 1, 2.5, 5, and 10 μM Hoechst-DBCO and 10 μM Hoechst 33258 for 1 h at 37 °C, and the cellular fluorescence was analyzed by flow cytometry. The results showed uptake of Hoechst-DBCO for all concentrations and an increase in fluorescence intensity as the concentration of Hoechst-DBCO increased in both cell lines, Figure S2A,B. To evaluate the influence of the linker-DBCO moiety on cellular uptake of Hoechst, we analyzed the fluorescence intensity of 10 μM Hoechst-DBCO and 10 μM Hoechst 33258 in CAL27 and HEK293 cells. The CAL27 cells showed a statistically significant but modest increase in fluorescence intensity for Hoechst 33258 (2429 ± 114.5) compared to Hoechst-DBCO (2198 ± 8.39), while the uptake of Hoechst 33258 was 3.7-fold higher than that of Hoechst-DBCO in HEK293 cells, Figure S2A,B. Thus, the results indicate that the uptake profile for Hoechst-DBCO is cell-line-dependent. In CAL27 cells, a 2.8- to 4.0-fold higher fluorescence intensity could be observed compared to HEK293 cells. In addition, Hoechst 33258 uptake was higher in both cell lines compared to Hoechst-DBCO. This suggests that the linker-DBCO moiety has a negative impact on cellular uptake; however, the extent to which this occurs may or may not be that drastic. The underlying reasons may be due to differences in cellular transport mechanisms, membrane permeability, cellular morphology, nuclear DNA content, and the efficiency of the compound to access the DNA minor groove.

The SPAAC reaction between Hoechst-DBCO and BDP FL azide was assessed in living CAL27 and HEK293 cells by flow cytometry. BDP FL azide was chosen because it is a small lipophilic molecule and has a neutral charge at physiological pH, which makes it passively permeable across cell membranes (Figure 2). To evaluate the intracellular click reaction, CAL27 and HEK293 cells pretreated with Hoechst-DBCO and untreated cells were treated with 1−10 μM BDP FL azide (Figure 3). The CAL27 cells pretreated with Hoechst-DBCO showed significantly higher fluorescence of BDP FL azide compared to cells treated with BDP FL azide alone (6873 ± 46.7 vs 986 ± 8.2, respectively), Figure S3A. HEK293 cells show a similar trend in fluorescence, Figure S3B. The analysis of Hoechst-DBCO fluorescence in CAL27 and HEK293 cells treated with 10 μM Hoechst-DBCO and different concentrations of BDP FL azide shows that the fluorescence of Hoechst-DBCO decreases significantly as the fluorescence of BDP FL azide increases, Figure S4A,B.

As a control experiment, CAL27 and HEK293 cells pretreated with 10 μM Hoechst 33258, 10 μM Hoechst-DBCO, and untreated cells were treated with 10 μM BDP FL azide. CAL27 and HEK293 cells pretreated with Hoechst-DBCO showed significantly higher fluorescence of BDP FL azide compared with cells treated with BDP FL azide alone or pretreated with Hoechst 33258 (20443 ± 1837 vs 4989 ± 287.4 vs 6534 ± 1785), respectively, Figure S5, suggesting greater residual activity due to the intracellular SPAAC reaction. In contrast, cells pretreated with Hoechst 33258 followed by BDP FL azide showed fluorescence intensities comparable to those treated with BDP FL azide alone, with no statistically significant difference, suggesting nonspecific binding and retention of the dye within the cells. When BDP FL azide enters cells, if unreacted, it may exit cells through passive diffusion or through efflux pumps or bind nonspecifically to intracellular proteins and membranes. Since BDP FL azide is a

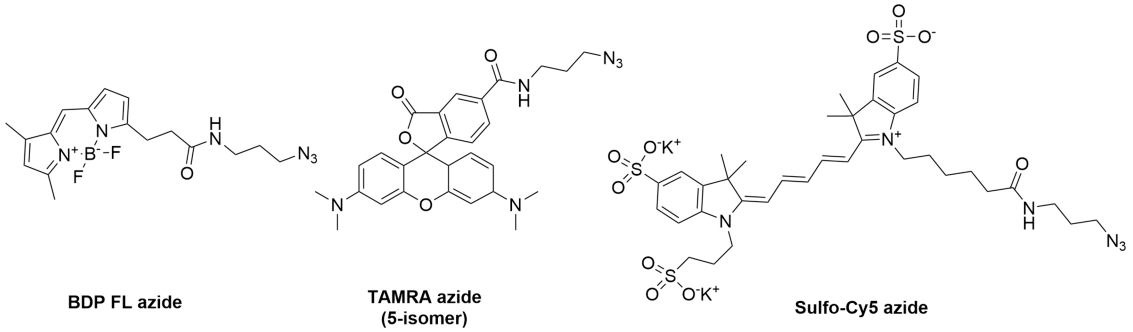

Figure 2. Chemical structures of BDP FL azide, TAMRA azide (5-isomer), and sulfo-Cy5 azide.

https://doi.org/10.1021/cbmi.5c00207
Chem. Biomed. Imaging XXXX, XXX, XXX−XXX

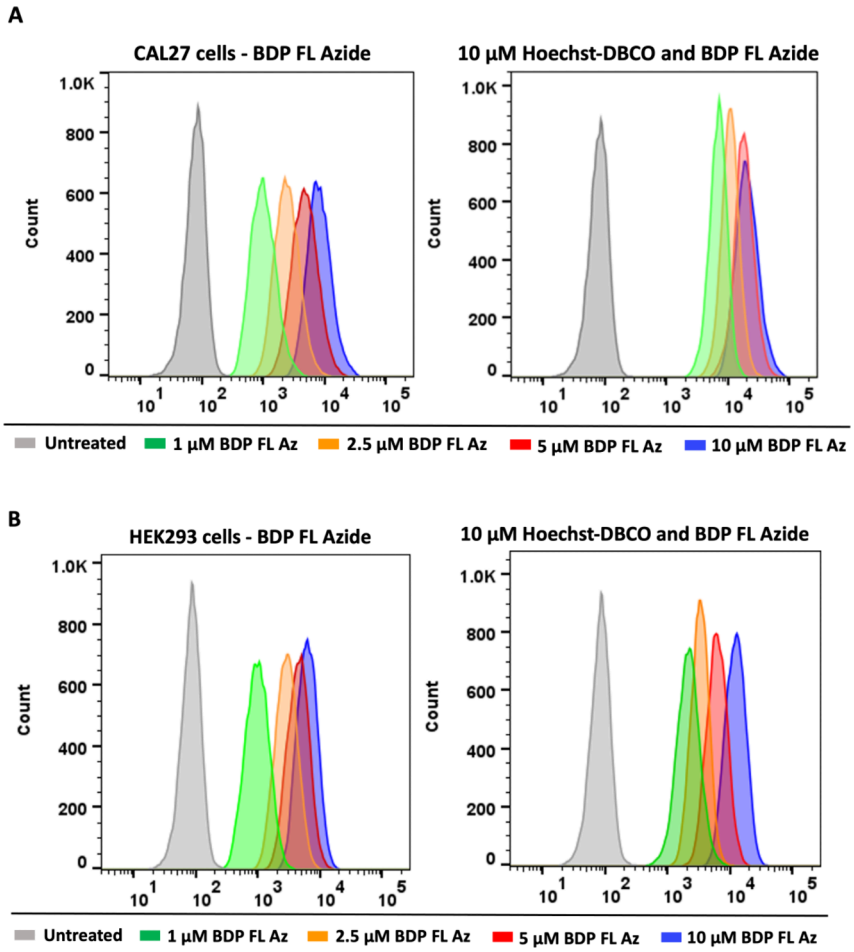

Figure 3. Cellular uptake of BDP FL azide analyzed by flow cytometry. (A) Flow cytometry analysis of CAL27 cells treated with 1, 2.5, 5, and 10 μM BDP FL azide, with or without pretreatment with 10 μM Hoechst-DBCO. (B) Flow cytometry analysis of HEK293 cells under the same conditions. Representative histogram plots illustrate fluorescence shifts indicative of BDP FL azide uptake and the successful click reaction.

fluorescent dye itself, it may contribute to the overall fluorescence signal within the cell, which is why the cells were treated with BDP FL azide alone in parallel to the experiment. This allowed us to estimate the nonspecific binding and deduce it from the fluorescence intensity of the SPAAC reaction. Based on the generated results, we were unfortunately not able to quantify the nuclear uptake as flow cytometry lacks the spatial resolution required to assess the intracellular distribution accurately.

Quantification of Hoechst-DBCO and Azides Using a Fluorescence-Based Assay

The cellular uptake of Hoechst-DBCO in CAL27 cells was quantified by using fluorescence. To quantify the cell uptake, the cells must be lysed in a way that ensures that the Hoechst fluorescence signal is recovered. Initially, Hoechst-DBCO was analyzed under different cell lysis conditions. 0.5 μM Hoechst-DBCO was mixed with cell extracts prepared with different lysis buffers, and the fluorescence was recorded after excitation at 352 nm. The lysis buffer that has optimal results with Hoechst-DBCO was 0.15 M NaCl + 1% SDS in 20 mM phosphate buffer, pH 7.0, and was used as a lysis buffer in this study, Figure S6. Ligasová and Koberna reported that the fluorescence signal intensity of bisbenzimidazole dyes depends on the pH and buffer composition.[23] The same study also reported the dependence of the fluorescence signal of bisbenzimidazole dyes and SDS concentrations.[23] SDS is an anionic detergent used to disrupt cell membranes and release cellular content, including DNA and proteins. The peak emission of Hoechst-DBCO fluorescence was observed at 495 nm, and the presence of CAL27 cells did not interfere with its fluorescence intensity, Figure S7. The addition of 1% SDS to the lysis buffer resulted in a 45-fold increase in the Hoechst-DBCO fluorescence intensity, Figure S8A, presumably due to the formation of micelles, which are known to increase the fluorescence of Hoechst 33258.[23]

The cells treated with 2.5, 5, and 10 μM Hoechst-DBCO presented an uptake of 24.70 ± 3.60 nM/mg protein, 184.6 ± 4.44 nM/mg protein, and 338.12 ± 23.25 nM/mg protein, respectively, Figures S8B and S9A. Analysis of Hoechst-DBCO concentration in cells treated with 10 μM Hoechst-DBCO for 1 h, followed by incubation in DMEM supplemented with 10% FBS for 1, 2, and 3 h, showed no statistically significant differences, Figure S9B. Our results showed that Hoechst-DBCO is well retained within the cells for 3 h, with no significant change in fluorescence intensity observed during this period. However, the results showed a significant difference in Hoechst-DBCO concentration immediately after treatment, compared with the cell concentration 1 h post-treatment. This highlights the importance of the washing steps with PBS and the incubation time with fresh medium to remove unbound Hoechst-DBCO.

https://doi.org/10.1021/cbmi.5c00207
Chem. Biomed. Imaging XXXX, XXX, XXX−XXX

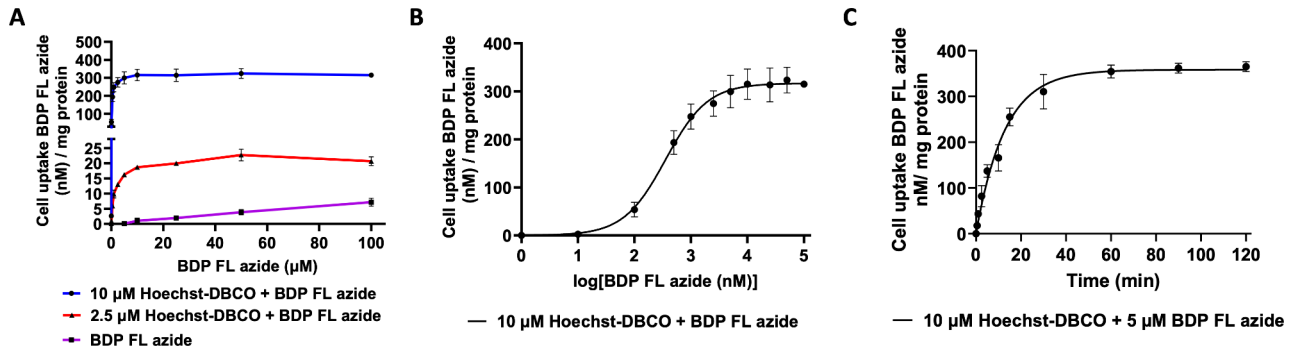

Figure 4. Analysis of SPAAC reactions of Hoechst-DBCO and BDP FL azide in the nucleus of live CAL27 cells. Cells pretreated with 2.5 and 10 μM Hoechst-DBCO for 1 h and untreated cells were treated with 10 nM to 100 μM BDP FL azide for 1 h at 37 °C. Cells were lysed, sonicated, centrifuged and the fluorescence intensity was analyzed in the supernatant. (A) Comparison of cellular uptake of BDP FL azide in cells pretreated with 2.5 and 10 μM Hoechst-DBCO, and untreated cells. (B) Dose−response curve of fluorescence intensity analysis of the SPAAC reaction of Hoechst-DBCO and BDP FL azide. (C) Single-phase association curve from the analysis of fluorescence intensity over time of SPAAC reactions between Hoechst-DBCO reacting with 5 μM BDP FL azide at 37 °C for 0.5−120 min. Data were obtained from n = 3 independent replicates, analyzed using GraphPad Prism, and reported as the mean ± standard deviation (STDEV).

Table 1. Reaction Rate and Efficiency for the SPAAC Reaction in the Nucleus of Live Cells

Hoechst-DBCO (μM)	azide	EC_{50} (nM)	$t_{1/2}$ (min)	E_{max} (nM)
10	BDP FL azide	0.358	8.904	358.4
10	TAMRA azide (5-isomer)	5.584	17.09	265.9

In this assay, quantification of Hoechst-DBCO uptake by CAL27 cells was based on total fluorescence and did not depend on the dye's fluorescence enhancement upon binding to nucleic acids. Instead, a lysis buffer was used to elute Hoechst-DBCO bound to DNA, with SDS in the buffer being responsible for amplifying the fluorescence signal. Furthermore, a sonication step was added to ensure the complete solubilization of the nuclear membranes.

To investigate the SPAAC reactions of Hoechst-DBCO and azides in the nucleus of live CAL27 cells, three different azides were selected based on their cell permeability profiles (Figure 2). Both BDP FL azide and TAMRA azide (5-isomer) are lipophilic molecules, highly fluorescent, photostable, providing strong signals suitable for detection, and can easily enter the cell by passive diffusion without the need for transporters.[24] BDP FL azide is characterized by a neutral charge at physiological pH, while TAMRA azide (5-isomer) provides zwitterionic properties under physiological conditions.[22] Furthermore, TAMRA azide (5-isomer) is known for a good intracellular distribution and diffusion. Sulfo-Cy5 azide is a far-red dye, negatively charged under physiological conditions, and highly hydrophilic with poor passive cell membrane permeability.

A dose−response analysis of the reaction between Hoechst-DBCO and BDP FL azide was performed to determine the half-maximal effective concentration (EC_{50}), defined as the concentration at which 50% of the available labeling sites are modified. Two Hoechst-DBCO concentrations, 2.5 and 10 μM, were tested against a range of BDP FL azide concentrations from 10 nM to 100 μM. Higher concentration of Hoechst-DBCO resulted in lower EC_{50} values, indicating increased binding efficiency and earlier saturation of labeling sites. CAL27 cells treated with 10 nM to 1 μM BDP FL azide alone showed cellular uptake of less than 100 pM/mg protein, while cells treated with 100 μM BDP FL azide showed an uptake of 6.70 ± 1.42 nM/mg protein, Table S1 and Figure S10. However, CAL27 cells pretreated with 10 μM Hoechst-DBCO and then exposed to 10 nM, 10 μM, and 100 μM BDP FL azide presented uptake levels of 2.60 ± 0.03 nM/mg protein, 315.04 ± 31.62 nM/mg protein, and 314.90 ± 5.66 nM/mg protein, respectively, Table S1. Notably, the cellular uptake of 10 μM BDP FL azide in cells pretreated with 10 μM Hoechst-DBCO was 208.6-fold higher compared with cells treated with BDP FL azide alone, Figure 4. In contrast, CAL27 cells pretreated with 10 μM Hoechst 33258, followed by BDP FL azide treatment, showed fluorescence intensities comparable to those treated with BDP FL azide alone, with no statistically significant difference, suggesting nonspecific binding and retention of the dye within the cells, Figure S12.

The interaction between Hoechst-DBCO and BDP FL azide was examined to assess its effect on the fluorescence intensity of the BDP FL azide. The SPAAC reaction between Hoechst-DBCO and BDP FL azide did not result in any enhancement of BDP FL azide fluorescence (Figure S13). Similarly, the addition of CAL27 cell lysate had no measurable impact on the BDP FL fluorescence intensity, Figure S14. Although both Hoechst-DBCO and BDP FL azide present emission wavelengths in close proximity (495 and 520 nm, respectively), the fluorescence intensity of BDP FL azide remained stable, regardless of whether it was measured alone or in combination with Hoechst-DBCO, Figure S14. Furthermore, the presence of Hoechst-DBCO in the supernatant did not influence BDP FL azide fluorescence, as shown in Figure S15.

To further investigate the reaction between Hoechst-DBCO and BDP FL azide, time-course studies were performed using 5 μM BDP FL azide. These experiments aimed to determine the kinetic parameters of the reaction, specifically, the half-life ($t_{1/2}$) and the maximal effect (E_{max}). The half-life ($t_{1/2}$) is defined as the time required for the fluorescence intensity to reach 50% of the maximum response observed between the baseline and saturation levels at the applied concentration. Additionally, the maximal fluorescence response (E_{max}) was calculated from the time-course data to assess the overall

https://doi.org/10.1021/cbmi.5c00207
Chem. Biomed. Imaging XXXX, XXX, XXX−XXX

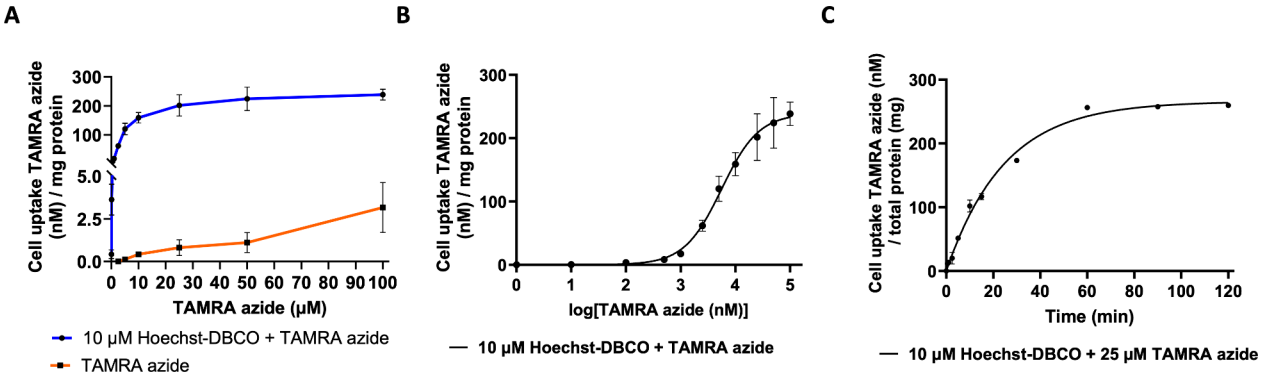

Figure 5. Analysis of SPAAC reactions of Hoechst-DBCO and TAMRA azide (5-isomer) in the nuclei of live CAL27 cells. Cells pretreated with 10 μM Hoechst-DBCO for 1 h and untreated cells were treated with 10 nM to 100 μM TAMRA azide (5-isomer) for 1 h at 37 °C. Following treatment, cells were lysed, sonicated, and centrifuged and the fluorescence intensity was analyzed in the supernatant. (A) Comparison of TAMRA azide (5-isomer) uptake in cells pretreated with 10 μM Hoechst-DBCO and untreated cells. (B) Dose−response curves from fluorescence intensity analysis of the supernatant from the SPAAC reaction of Hoechst-DBCO and TAMRA azide (5-isomer). (C) One-phase association curves from time course fluorescence intensity analysis of SPAAC reactions between Hoechst-DBCO and 25 μM TAMRA azide (5-isomer) for 0.5−120 min. Data were obtained from n = 3 independent replicates, analyzed using GraphPad Prism, and reported as the mean ± standard deviation (STDEV).

reaction efficiency. The results of these analyses are summarized in Table 1.

To quantify TAMRA azide (5-isomer) uptake and the SPAAC reaction, cells pretreated with 10 μM Hoechst-DBCO and treated with 10 nM, 10 μM, and 100 μM TAMRA azide (5-isomer) showed uptake values of 0.43 ± 0.25 nM/mg protein, 159.05 ± 18.21 nM/mg protein, and 238.64 ± 18.56 nM/mg protein, respectively (Figure 5). In contrast, cells treated with 10 nM to 25 μM TAMRA azide (5-isomer) alone showed minimal cellular uptake (<1 nM), and cells treated with 100 μM TAMRA azide (5-isomer) alone showed an uptake of 3.17 ± 1.46 nM/mg protein, Table S2. The cellular uptake of 10 μM TAMRA azide (5-isomer) in cells pretreated with 10 μM Hoechst-DBCO was 369.88-fold higher than that in cells treated with TAMRA azide (5-isomer) alone. The reactions between Hoechst-DBCO and TAMRA azide (5-isomer) were further investigated using a time course with 25 μM TAMRA azide (5-isomer) to determine the $t_{1/2}$ and E_{max} values, Table 1.

The results showed significant differences in the EC_{50}, $t_{1/2}$, and E_{max} values between BDP FL azide and TAMRA azide (5-isomer) upon reaction with Hoechst-DBCO. The cellular uptake of BDP FL azide and TAMRA azide (5-isomer) in cells without any prior treatment showed that BDP FL azide presented higher uptake compared to TAMRA azide (5-isomer). The higher cellular uptake of BDP FL azide can be attributed to its smaller size, high lipophilicity, and lower polarity. These characteristics facilitate the passive diffusion of BDP FL azide across the cellular membrane. In contrast, TAMRA azide (5-isomer) presents higher polarity and frequently exists in a charged or zwitterionic form under physiological conditions, which reduces its membrane permeability. Although the rhodamine core structure contributes to its polarity, TAMRA azide (5-isomer) still shows effective cellular uptake; however, its increased polarity compared to more hydrophobic dyes can slow passive diffusion across the cell membrane.

The SPAAC reaction between Hoechst-DBCO and sulfo-Cy5 azide was also evaluated. Cells treated with sulfo-Cy5 azide alone showed minimal uptake (<0.05 nM/mg protein) at all concentrations tested (1−100 μM), whereas cells pretreated with 10 μM Hoechst-DBCO, followed by 100 μM sulfo-Cy5 azide, showed an uptake of 0.55 ± 0.07 nM/mg protein, Table S3 and Figure S19. Sulfo-Cy5, which contains three sulfonate groups, is highly water-soluble and exhibits poor membrane permeability under physiological conditions due to its anionic charge. Its hydrophilicity and strong negative charge prevent passive diffusion across the cell membrane, resulting in low cellular uptake, unless internalization occurs via active processes such as endocytosis. These results confirm the assay selectivity. This assay was designed to measure intracellular SPAAC reactions in living cells. The low uptake of sulfo-Cy5 azide, a cell membrane impermeable compound, suggests that the assay is measuring specific intracellular reactions, and the results are not influenced by Hoechst-DBCO and azides reacting in the medium or extracellular spaces.

The fluorescence intensity analyses of Hoechst-DBCO before and after treatment with different concentrations of BDP FL azide and TAMRA azide (5-isomer) showed a gradual decrease in fluorescence intensity (Table S4). However, this behavior was not observed in the fluorescence intensity of cells treated with Hoechst 33258 and different concentrations of BDP FL azide and TAMRA azide (5-isomer). In this case, the fluorescence intensity of Hoechst 33258 remains the same regardless of the BDP FL azide and TAMRA azide (5-isomer) concentration. Hoechst dyes can lose their fluorescence when their chemical structure is altered. The SPAAC reaction covalently binds DBCO-modified Hoechst to BDP FL azide via a triazole ring. This new chemical environment can disrupt the electronic structure of the Hoechst fluorophore, leading to a decrease and loss of fluorescence. In cells treated with 100 μM BDP FL azide or TAMRA azide (5-isomer), the concentration of Hoechst-DBCO decreases by approximately 50% compared to the initial concentration.

In addition, cell viability studies employing a water-soluble tetrazolium-1 (WST-1) assay showed that 10 μM Hoechst-DBCO, 100 μM BDP FL azide, 100 μM TAMRA azide (5-isomer), and 100 μM sulfo-Cy5 azide, incubated for 4 h, did not affect the cell viability of CAL27 cells, Figure S21.

SPAAC Reaction and Fluorescence Microscopy

We next explored the SPAAC reaction in the nucleus by using fluorescence microscopy. CAL27 cells were pretreated with 10 μM Hoechst-DBCO, followed by treatment with 1 μM BDP

https://doi.org/10.1021/cbmi.5c00207
Chem. Biomed. Imaging XXXX, XXX, XXX−XXX

FL azide, 1 μM TAMRA azide (5-isomer), and 1 μM sulfo-Cy5 azide. The Hoechst-DBCO signal is present only in the nucleus (Figures S22, 6, and 7), while the BDP FL azide and

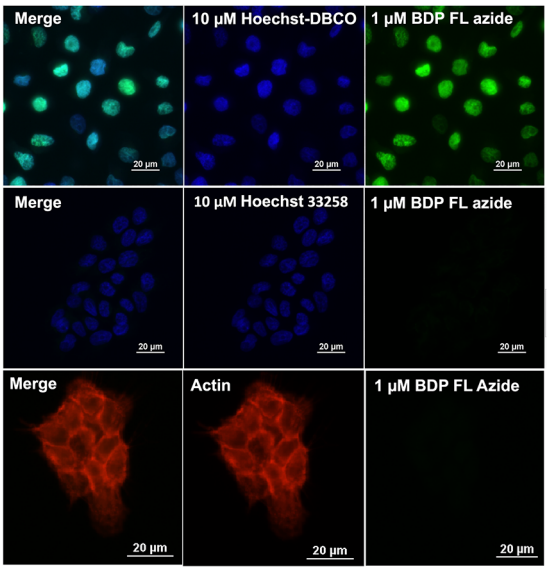

Figure 6. Fluorescence microscopy images of SPAAC reactions between Hoechst-DBCO and BDP FL azide in fixed cells. CAL27 cells were treated with 10 μM Hoechst-DBCO or Hoechst 33258 for 60 min at 37 °C, followed by the reaction with 1 μM BDP FL azide for 60 min at 37 °C. Hoechst-DBCO or Hoechst 33258 labeled the nucleus (blue), while BDP FL azide labeled the nucleus (green). As a control, cells were treated with 10 μM Hoechst 33258 followed by 1 μM BDP FL azide. Cells treated only with 1 μM BDP FL azide were counterstained with Alexa Fluor 594 phalloidin to label actin in the cytoplasm (red).

TAMRA azide (5-isomer) signal appears to be present diffusely throughout the cytosol and nucleus of living cells (Figure S22); however, in fixed cells, it is suggested to be present only in the nucleus, Figures 6 and 7. The results observed in living cells align with previous studies reported by Makanai et al., showing dual accumulation of TAMRA azide (5-isomer) in the nucleus and mitochondria.[25]

As a control, cells treated with Hoechst 33258, followed by BDP FL azide or TAMRA azide (5-isomer), were analyzed. The results showed the fluorescence signal from Hoechst 33258 in the nucleus but no signal of BDP FL azide or TAMRA azide (5-isomer) in the nucleus or other part of the cells, suggesting that the fluorescence present in the cells that express DBCO in the nucleus is a result of the SPAAC reaction, Figures 6 and 7. Furthermore, in cells treated only with 1 μM BDP FL azide, no signal was detected; the cells were also stained with actin to improve visualization, Figure 6. We also tested sulfo-Cy5 azide, with cells that express DBCO in the nucleus, and no signal of sulfo-Cy5 azide was detected, Figure 7. Sulfo-Cy5 azide is impermeable in the majority of cell lines.

Additionally, the SPAAC reaction of 10 μM Hoechst-DBCO with 0.5, 1, 2.5, and 25 μM BDP FL azide or 0.5, 2.5, 10, and 25 μM TAMRA azide (5-isomer) was evaluated using fluorescence microscopy, Figures 8 and 9. A significant SPAAC reaction was observed with 0.5 μM BDP FL azide, and the reaction becomes saturated with 2.5 μM BDP FL azide, while TAMRA azide (5-isomer) showed few reactions

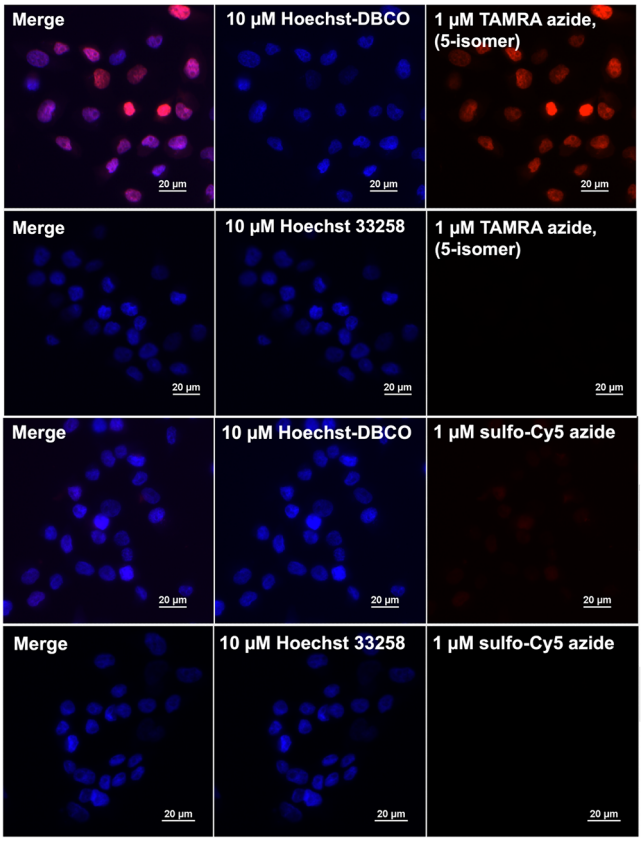

Figure 7. Fluorescence microscopy images of SPAAC reactions of Hoechst-DBCO and TAMRA azide (5-isomer) in fixed cells. CAL27 cells were treated with 10 μM Hoechst-DBCO or Hoechst 33258 for 60 min at 37 °C, followed by the reaction with 1 μM TAMRA azide (5-isomer) or 1 μM sulfo-Cy5 azide for 60 min at 37 °C. Hoechst-DBCO or Hoechst 33258 labeled nucleus (blue), TAMRA azide (5-isomer) labeled nucleus (red). As a control, cells were treated with 10 μM Hoechst 33258, followed by 1 μM TAMRA azide (5-isomer) or 1 μM sulfo-Cy5 azide.

with 0.5 μM TAMRA azide (5-isomer) and becomes saturated with 25 μM.

Evaluation of a Radiotracer Candidate for Intracellular SPAAC Reactions

Finally, the assay was validated using an in-house developed radiotracer. A comparison of the intracellular accumulation of [^{18}F]FDG-N_3 in CAL27 cells treated with 10 μM Hoechst-DBCO and untreated showed a statistically significant difference, Figure 10. Specifically, the [^{18}F]FDG-N_3 uptake values were 0.73% ± 0.05 vs 0.17% ± 0.03 at 1 h and 0.55% ± 0.02 vs 0.17% ± 0.01 at 2 h for Hoechst-DBCO treated and untreated cells, respectively, suggesting higher uptake due to intracellular SPAAC. Cells treated with 0.5 MBq [^{18}F]FDG-triazol-DBCO-Hoechst for 1 and 2 h showed an increase in cellular uptake over time from 0.51% ± 0.02 after 1 h to 1.05% ± 0.02 after 2 h of incubation. The reaction between Hoechst-DBCO and [^{18}F]FDG-N_3 in vitro for 2 h was sufficient to react all azides in the solution. In vitro comparisons of targeted and pretargeted uptake using click chemistry are important to optimize reaction conditions and specificity and for selecting the best strategy for future *in vivo* applications. In the targeted approach, [^{18}F]FDG-triazol-DBCO-Hoechst reaches the nucleus through passive diffusion, while in the pretargeted approach, the time required for [^{18}F]FDG-N_3 to enter cells via

https://doi.org/10.1021/cbmi.5c00207
Chem. Biomed. Imaging XXXX, XXX, XXX−XXX

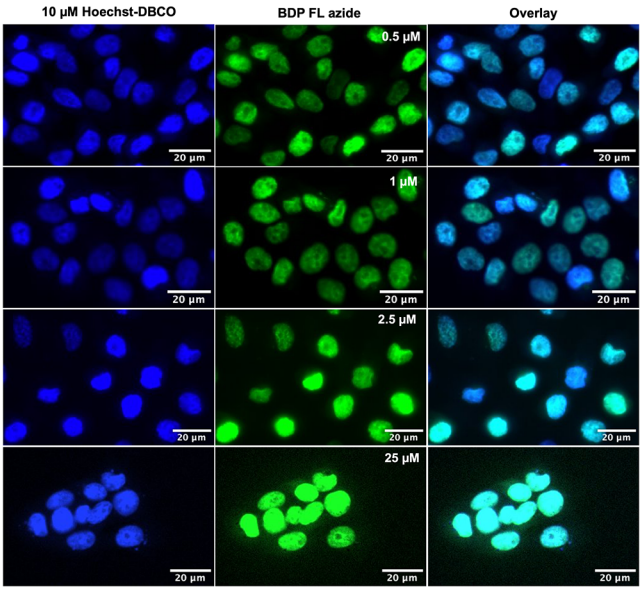

Figure 8. Fluorescence microscopy images of SPAAC reactions between Hoechst-DBCO and BDP FL azide in fixed cells. CAL27 cells were treated with 10 μM Hoechst-DBCO, followed by the reaction with 0.5, 1, 2.5, and 25 μM BDP FL azide. Hoechst-DBCO labeled nucleus (blue), and BDP FL azide labeled nucleus (green).

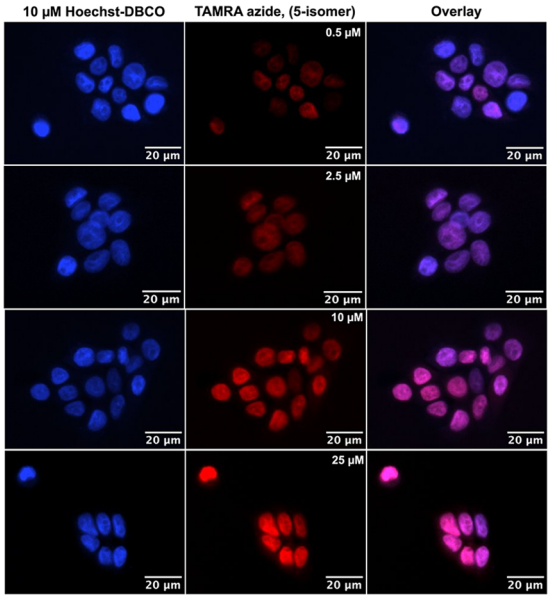

Figure 9. Fluorescence microscopy images of SPAAC reaction between Hoechst-DBCO and TAMRA azide (5-isomer) in fixed cells. CAL27 cells were treated with 10 μM Hoechst-DBCO, followed by the reaction with a 0.5, 2.5, 10, and 25 μM TAMRA azide (5-isomer). Hoechst-DBCO labeled nucleus (blue), and TAMRA azide (5-isomer) labeled nucleus (red).

GLUT-mediated transport and cross the nuclear membrane was evaluated.

Additionally, a competitive assay was performed using cold FDG to assess the specificity of the uptake. The use of 18 nM cold FDG decreased the rate of uptake of [^{18}F]FDG-N$_3$ by 45%. Since FDG is transported into cells primarily via glucose transporter proteins (GLUTs), these transporters enable facilitated diffusion of glucose analogues,[26] such as FDG and [^{18}F]FDG-N$_3$, across the cell membrane, and the observed

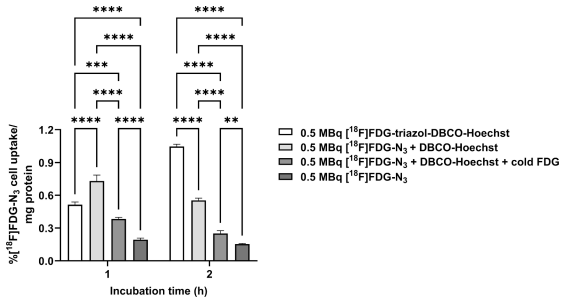

Figure 10. Intracellular SPAAC reaction of Hoechst-DBCO with [^{18}F]FDG-N$_3$ in CAL27 cells. Cells were pretreated with 10 μM Hoechst-DBCO for 1 h at 37 °C. After incubation, cells were washed and incubated with 0.5 MBq of [^{18}F] FDG-N$_3$ for 1 and 2 h at 37 °C. For the control, the cells were incubated only with [^{18}F]FDG-N$_3$ or with the conjugate [^{18}F]FDG-triazol-DBCO-Hoechst. Data are presented as mean ± standard deviation. The experiment was performed in triplicate. Statistical analysis was performed with two-way ANOVA and Tukey's multiple comparison test, with p-value < 0.05 considered as the level of statistical significance. **p < 0.01, ***p < 0.001, ****p < 0.0001.

competition further supports GLUT-mediated radiotracer uptake.

CONCLUSIONS

In summary, the main idea of this study was to develop an *in vitro* assay that can rapidly investigate the uptake and SPAAC click reaction of new compounds used in the development of new approaches based on pretargeted PET imaging. It was demonstrated that Hoechst-DBCO can effectively transport DBCO to the nucleus. Its high affinity and specificity for DNA make Hoechst a good targeting moiety. Uptake studies in CAL27 cells confirmed that Hoechst-DBCO is retained intracellularly well for up to 3 h, with no significant changes in fluorescence intensity observed during this period, indicating strong cellular retention. This allowed us to successfully investigate bioorthogonal SPAAC click reactions in living cells and evaluate the intracellular uptake of new compounds. Hoechst-DBCO therefore serves as a valuable tool for monitoring SPAAC reactions at the intracellular level. Overall, Hoechst-DBCO proved to be a promising agent from the combined assessment of cellular uptake and intracellular SPAAC reactivity. Our approach addresses the need for rapid and sensitive methods to study intracellular click chemistry in living cells.

ASSOCIATED CONTENT

Supporting Information

The Supporting Information is available free of charge at https://pubs.acs.org/doi/10.1021/cbmi.5c00207.

Additional figures, experimental details, and NMR chart (PDF)

AUTHOR INFORMATION

Corresponding Author

Anu J. Airaksinen − *Turku PET Centre, Turku University Hospital and University of Turku, Turku FI-20520, Finland; Department of Chemistry, University of Turku, Turku FI-20520, Finland;* orcid.org/0000-0002-5943-3105; Email: anu.airaksinen@utu.fi

https://doi.org/10.1021/cbmi.5c00207
Chem. Biomed. Imaging XXXX, XXX, XXX−XXX

Authors

Luciana Kovacs − *Turku PET Centre, Turku University Hospital and University of Turku, Turku FI-20520, Finland; Department of Chemistry, University of Turku, Turku FI-20520, Finland*

Risto Savela − *Turku PET Centre, Turku University Hospital and University of Turku, Turku FI-20520, Finland; Department of Chemistry, University of Turku, Turku FI-20520, Finland*

Jelena Matovic − *Department of Chemistry, University of Helsinki, Helsinki FI-00014, Finland*

Tatsiana Auchynnikava − *Turku PET Centre, Turku University Hospital and University of Turku, Turku FI-20520, Finland; Department of Chemistry, University of Turku, Turku FI-20520, Finland;* orcid.org/0000-0001-8940-6012

Filip S. Ekholm − *Department of Chemistry, University of Helsinki, Helsinki FI-00014, Finland;* orcid.org/0000-0002-4461-2215

Complete contact information is available at: https://pubs.acs.org/10.1021/cbmi.5c00207

Author Contributions

This manuscript was written through contributions of all authors. All authors have given approval to the final version of the manuscript.

Funding

This research was supported by the Research council of Finland (decision number 343608), Jane and Aatos Erkko Foundation, and Cancer Foundation of Finland (synthesis of the FDG-Az starting material).

Notes

The authors declare no competing financial interest.

■ ACKNOWLEDGMENTS

The authors would like to acknowledge Leon Luckenbach for his technical assistance with cell uptake studies. Cytometry and fluorescence microscopy was performed at the Cell Imaging and Cytometry Core, the Finnish Advanced Microscopy Node of EuroBioimaging Finland at Turku Bioscience Centre (Turku, Finland).

■ REFERENCES

(1) Baskin, J. M.; Prescher, J. A.; Laughlin, S. T.; Agard, N. J.; Chang, P. V.; Miller, I. A.; Lo, A.; Codelli, J. A.; Bertozzi, C. R. Copper-Free click chemistry for dynamic in vivo imaging. *Proc. Natl. Acad. Sci. U.S.A.* **2007**, *104* (43), 16793−16797.

(2) Derks, Y. H. W.; Rijpkema, M.; Amatdjais-Groenen, H. I. V.; Loeff, C. C.; de Roode, K. E.; Kip, A.; Laverman, P.; Lütje, S.; Heskamp, S.; Löwik, D. W. P. M. Strain-promoted azide−alkyne cycloaddition-based PSMA-targeting ligands for multimodal intraoperative tumor detection of prostate Cancer. *Bioconjug Chem.* **2022**, *33* (1), 194−205.

(3) Nikic, I.; Kang, J. H.; Girona, G. E.; Aramburu, I. V.; Lemke, E. A. Labeling proteins on live mammalian cells using click chemistry. *Nat. Protoc* **2015**, *10* (5), 780−791.

(4) Beatty, K. E.; Fisk, J. D.; Smart, B. P.; Lu, Y. Y.; Szychowski, J.; Hangauer, M. J.; Baskin, J. M.; Bertozzi, C. R.; Tirrell, D. A. Live-cell imaging of cellular proteins by a strain-promoted azide-alkyne cycloaddition. *ChemBioChem.* **2010**, *11* (15), 2092−2095.

(5) Rondon, A.; Degoul, F. Antibody Pretargeting based on bioorthogonal click chemistry for cancer imaging and targeted radionuclide therapy. *Bioconjug Chem.* **2020**, *31* (2), 159−173.

(6) Sarrett, S. M.; Keinänen, O.; Dayts, E. J.; Dewaele-Le Roi, G.; Rodriguez, C.; Carnazza, K. E.; Zeglis, B. M. Inverse electron demand diels−alder click chemistry for pretargeted pet imaging and radioimmunotherapy. *Nat. Protoc* **2021**, *16*, 3348−3381.

(7) Sletten, E. M.; Bertozzi, C. R. Bioorthogonal chemistry: fishing for selectivity in a sea of functionality. *Angew. Chem., Int. Ed.* **2009**, *48*, 6974−6998.

(8) Kolb, H. C.; Finn, M. G.; Sharpless, K. B. Click Chemistry: Diverse Chemical Function from a Few Good Reactions. *Angew. Chem., Int. Ed.* **2001**, *40*, 2004−2021.

(9) Castelvecchi, D.; Ledford, H. Chemists who invented revolutionary 'click' reactions win nobel. *Nature* **2022**, *610*, 242−243.

(10) Bauer, D.; Cornejo, M. A.; Hoang, T. T.; Lewis, J. S.; Zeglis, B. M. Click chemistry and radiochemistry: an update. *Bioconjugate Chem.* **2023**, *34* (11), 1925−1950.

(11) Meyer, J. P.; Adumeau, P.; Lewis, J. S.; Zeglis, B. M. Click chemistry and radiochemistry: the first 10 years. *Bioconjugate Chem.* **2016**, *27* (12), 2791−2807.

(12) Agard, N. J.; Prescher, J. A.; Bertozzi, C. R. A Strain-promoted [3 + 2] azide-alkyne cycloaddition for covalent modification of biomolecules in living systems. *J. Am. Chem. Soc.* **2004**, *126* (46), 15046−15047.

(13) Kim, E.; Koo, H. Biomedical applications of copper-free click chemistry: in vitro, in vivo, and ex vivo. *Chem. Sci.* **2019**, *10* (34), 7835−7851.

(14) Murrey, H. E.; Judkins, J. C.; Am. Ende, C. W.; Ballard, T. E.; Fang, Y.; Riccardi, K.; Di, L.; Guilmette, E. R.; Schwartz, J. W.; Fox, J. M.; Johnson, D. S. Systematic evaluation of bioorthogonal reactions in live cells with clickable halotag ligands: implications for intracellular imaging. *J. Am. Chem. Soc.* **2015**, *137* (35), 11461−11475.

(15) Lang, K.; Chin, J. W. Cellular incorporation of unnatural amino acids and bioorthogonal labeling of proteins. *Chem. Rev.* **2014**, *114* (9), 4764−4806.

(16) Yao, J. Z.; Uttamapinant, C.; Poloukhtine, A.; Baskin, J. M.; Codelli, J. A.; Sletten, E. M.; Bertozzi, C. R.; Popik, V. V.; Ting, A. Y. Fluorophore targeting to cellular proteins via enzyme-mediated azide ligation and strain-promoted cycloaddition. *J. Am. Chem. Soc.* **2012**, *134* (8), 3720−3728.

(17) Müggenburg, F.; Müller, S. Azide-Modified Nucleosides as Versatile Tools for Bioorthogonal Labeling and Functionalization. *Chem. Rec.* **2022**, *22* (5), No. e202100322.

(18) Ren, X.; El-Sagheer, A. H.; Brown, T. Azide and trans-Cyclooctene dUTPs: Incorporation into DNA Probes and fluorescent click-labelling. *Analyst* **2015**, *140* (8), 2671−2678.

(19) Zhou, Z.; Cironi, P.; Lin, A. J.; Xu, Y.; Hrvatin, S.; Golan, D. E.; Silver, P. A.; Walsh, C. T.; Yin, J. Genetically encoded short peptide tags for orthogonal labelling by sfp and acps phosphopantetheinyl transferases. *ACS Chem. Biol.* **2007**, *2* (5), 337−346.

(20) Bucevicius, J.; Gerasimaite, R.; Kostiuk, G.; Lukinavicius, G. *Fluorescent rhodamine dyes with enhanced cell permeability*. https://worldwide.espacenet.com/patent/search?q=pn%3DWO2021160732A1 (accessed Sep 24, 2025).

(21) Auchynnikava, T.; Matovic, J.; Kovacs, L.; Liljenback, H.; Imlimthan, S.; Dillemuth, P.; Novotna, D.; Rajander, J.; Sarparanta, M.; Li, X.-G.; Roivainen, A.; Ekholm, F.; Airaksinen, A. J. Radiolabeling of carborane via [18F]FDG-Az click chemistry: synthesis and biological evaluation. *Nuclear Medicine and Biology* **2025**, *150-151*, 109208 Supplement.

(22) Ranjan, N.; Kellish, P.; King, A.; Arya, D. P. Impact of linker length and composition on fragment binding and cell permeation: story of a Bisbenzimidazole dye fragment. *Biochemistry* **2017**, *56* (49), 6434−6447.

(23) Ligasová, A.; Koberna, K. Quantification of fixed adherent cells using a strong enhancer of the fluorescence of DNA dyes. *Sci. Rep.* **2019**, *9*, 8701.

(24) Cunningham, C. W.; Mukhopadhyay, A.; Lushington, G. H.; Blagg, B. S. J.; Prisinyano, T. E.; Krise, J. P. Uptake, distribution and diffusivity of reactive fluorophores in cells implications toward target identification. *Mol. Pharm.* **2010**, *7* (4), 1301−1310.

(25) Makanai, H.; Mochizuki, D.; Nishihara, T.; Tanabe, K. Hoechst modification by strain-promoted azide-alkynecycloaddition for transport of functional molecules into the cell nucleus. *Bioorg. Med. Chem. Lett.* **2024**, *112*, No. 129916.
(26) Salas, J. R.; Clark, P. M. Signaling pathways that drive ^{18}F-FDG accumulation in cancer. *J. Nucl. Med.* **2022**, *63* (5), 659−663.

NOTE ADDED AFTER ASAP PUBLICATION

Reference 21 was added after this paper was published ASAP on December 29, 2025. The revised version was reposted on January 5, 2026.

https://doi.org/10.1021/cbmi.5c00207
Chem. Biomed. Imaging XXXX, XXX, XXX−XXX